

We are IntechOpen, the world's leading publisher of Open Access books Built by scientists, for scientists

4,800

Open access books available

122,000

International authors and editors

135M

Downloads

Our authors are among the

154

Countries delivered to

TOP 1%

most cited scientists

12.2%

Contributors from top 500 universities



WEB OF SCIENCE™

Selection of our books indexed in the Book Citation Index
in Web of Science™ Core Collection (BKCI)

Interested in publishing with us?
Contact book.department@intechopen.com

Numbers displayed above are based on latest data collected.
For more information visit www.intechopen.com



Hysteresis Behavior of Pre-Strained Shape Memory Alloy Wires Subject to Cyclic Loadings: An Experimental Investigation

Shahin Zareie and Abolghassem Zabihollah

Abstract

Shape memory alloys (SMAs) are a class of smart materials with the ability to recover their initial shape after releasing the applied load and experiencing a relatively large amount of strain. However, sequential loading and unloading which is an unavoidable issue in many applications significantly reduces the strain recovery of SMA wires. In the present work, experimental tests have been performed to study the pre-strain effect of SMA wires on hysteresis behavior of SMA under cyclic loadings. The effects of cyclic loading on austenite and martensite properties have been investigated. SMA wires with diameter of 1.5 mm and length of 560 mm subjected to about 1000 cycles show about 3 mm residual deformation, which is approximately equal to 0.5% residual strain. It is observed that applying 1.7% pre-strain on the SMA wire fully eliminates the residual strain due to cyclic loading.

Keywords: shape memory alloy, cyclic loading, pre-strained, residual deformation

1. Introduction

Stability and failure control of structures are of the major challenges for civil structures in which the loading conditions are cyclic in nature, including harbor and offshore structures. In the past decades, a variety of active control mechanisms have been developed to ensure the stability of such structures [1]. However, active control mechanisms are relatively complex, requiring expensive and professional maintenance which are not always accessible. Therefore, for many structures, passive stability control mechanisms are preferred. Shape memory alloys (SMAs), due to their unique ability to recover their initial shape after releasing the applied load, are promising materials for energy absorption and ensuring the stability of structure under relatively large strain [2–7]. However, it is understood that the cyclic loading may highly influence the strain recovery property, superelasticity, of SMAs [8]. This phenomenon has been widely investigated by researchers in smart structure communities.

Zhang et al. [9] developed a low cycle fatigue criterion for superelasticity of SMAs considering thermomechanical coupling. They concluded that increasing strain rate decreases the fatigue lifetime in SMAs. A micromechanical model to describe the cyclic deformation of polycrystalline NiTi under different

thermomechanical conditions has been proposed by [10]. Wang et al. [11] proposed a novel structural building element integrated with SMA material to show the capability of SMA-based element in re-centering and energy dissipation of the structure after severe displacement.

Chemisky et al. [12] proposed an analytical model to describe the effects of cyclic loading at high temperature on SMAs behavior. Recently, remarkable researches have been performed to study the different parameters related to cyclic loadings on SMAs' behavior. Kan et al. [13] studied the effect of strain rate on uniaxial deformation of NiTi. Soul et al. [14] investigated the effect of loading frequency on the damping capacity of NiTi wires and concluded that loading frequency above 0.01 Hz significantly reduces the damping capacity of SMA wires. Des Roches et al. [15] evaluated the change in superelasticity of bar and wires made of NiTi under cyclic loading.

The present work aims to investigate the effects of pre-strained SMA wires under cyclic loading conditions on force-displacement behavior, particularly austenite and martensite phases, of SMAs. Experimental tests have been conducted to study the effect of the number of cycles, frequency of loading, and the pre-straining on hysteresis behavior of SMA wires under cyclic loadings.

2. Modeling superelasticity effect of SMA

When the temperature is equal to or greater than the austenitic finish temperature ($T \geq A_f$), SMA materials exhibit the superelasticity effect. **Figure 1** shows the stress-strain curve for loading and unloading of an SMA material. In the loading phase, there are two parts: linear and plastic, whereas in the unloading process, the material exhibits three portions, huge stress reduction with negligible strain reduction, huge strain reduction with a small amount of stress, and finally linear stress-strain reduction. It is noted that the area under the stress-strain curve describes the energy dissipation property of the SMA when loading and unloading. For an SMA rod with cross section (A) subjected to the axial loading (F), the stress

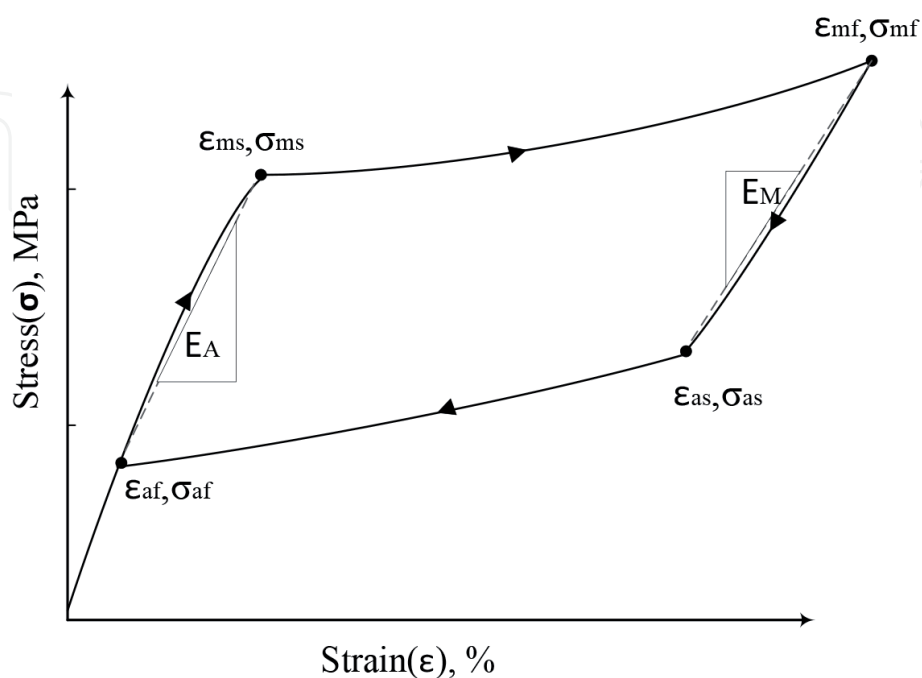


Figure 1.
The schematic diagram of the superelasticity in SMA.

is given by $\sigma = F/A$. Neglecting thermal expansion, the stress-strain of the SMA rod is computed as [16, 17]:

$$\sigma - \sigma_0 = E(\varepsilon - \varepsilon_0) + \Omega(\xi - \xi_0) \quad (1)$$

where $0 \leq \xi \leq 1$ indicates martensite fraction which is equal to zero for fully austenite phase and 1 for fully martensite. The term Ω is the transformation coefficient. Considering initial state as $\sigma_0 = \varepsilon_0 = 0$, $\xi_0 = 0$ and noting that after full phase transformation the material returns to zero stress, the transformation coefficient may be defined as a function of residual strain, $\Omega = E \varepsilon_r$. Therefore, the stress-strain relations for SMA can be expressed as:

$$\sigma - \sigma_0 = E(\varepsilon - \varepsilon_0) + \varepsilon_r E(\xi - \xi_0) \quad (2)$$

Eq. (2) can be modified for each region, for example, in the linear elastic region where the material is in full austenite phase ($\xi = 0$); Eq. (2) is given as:

$$\sigma = \varepsilon_r \varepsilon E \quad (3)$$

where E_A indicates the modulus of elasticity in austenite phase; similarly, for linear unloading stage where the material is in full martensite phase, modulus of elasticity is defined by E_M . For other regions, modulus of elasticity is a combination of E_A and E_M as the following [16, 17]:

$$E = E_A + (E_M - E_A)\xi \quad (4)$$

Further unloading beyond this point produces a linear elastic behavior to zero stress-strain. For further description on stress-strain relationships for superelasticity effect, one may refer to the book written by [16]. However, one may note that in the above expression, the effect of the number of loading/unloading cycles and pre-straining is not taken into consideration. The following sections provide a thorough study, particularly experimentally, on the effects of cyclic loading and pre-straining on stress-strain behavior of SMA materials.

3. Experimental tests

Experimental tests have been conducted using a universal testing machine—MTS model 370.5 with 500 kN loading capacity, 150 mm dynamic stroke, and 0.1–1 Hz loading frequency as shown in **Figure 2**. The SMA wire specimen of 560 mm length with 1.5 mm diameter made of NiTi has been subjected to cyclic tensile loadings. The material properties of NiTi wire, manufactured by Confluent Medical Technologies Company, are given in **Table 1**. Due to the small diameter of the specimen, each plate is clamped by the top and bottom grippers of the MTS loading machine, as shown in **Figure 3**. Loading frequencies, initial tensile load, loading rates, and the number of cycles have been predefined in the MTS machine for each test.

3.1 Single cycle loading and unloading test

In order to determine the force-displacement response curve for SMA specimen, a NiTi wire described above has been tested at room temperature with a quasi-static loading/unloading, with the period of 20 s and maximum amplitude 12 mm, as



Figure 2.
The MTS loading frame machine and its accessories.

Physical properties	Value
Melting point (°C)	1310
Density (g/cm ³)	6.5
Electrical resistivity (μ ohm-cm)	82
Modulus of elasticity (GPa)	41–75
Coefficient of thermal expansion (/°C)	11×10^{-6}
Ultimate tensile strength (MPa)	~1070
Total elongation	~10%
Straight length (mm)	560
Diameter (mm)	1.5

Table 1.
The properties of NiTi shape memory alloy.

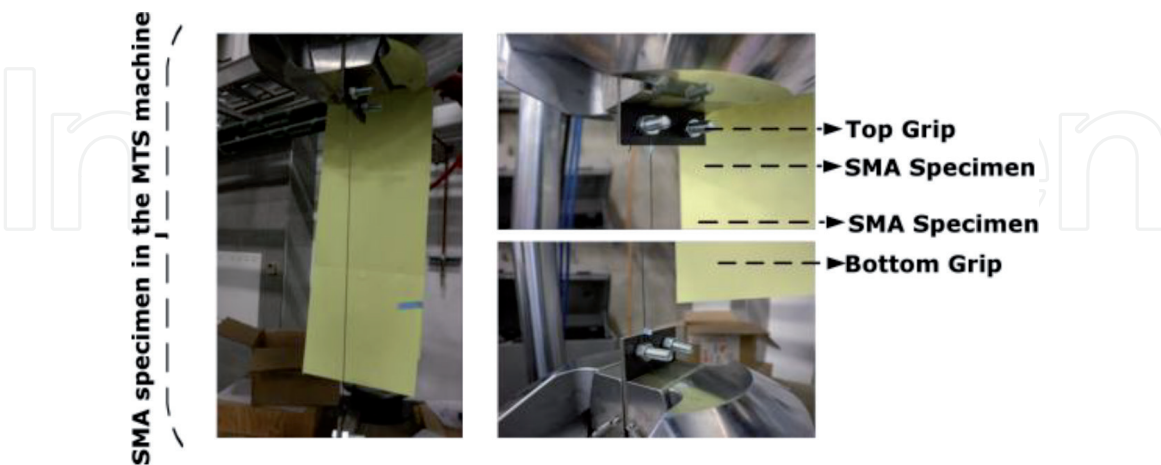


Figure 3.
The experimental setup for gripping the SMA specimen.

presented in **Figure 4**. Then, the test specimen is subjected to a cyclic load with 1000 cycles in which the period and maximum amplitude for the first cycle is 1.4 s and 20 mm, correspondingly, as shown in **Figure 5**. After completing 1000 cycles, the specimen is subjected again to the quasi-static load given in **Figure 4**. The force-displacement behavior of the specimen under the first quasi-static load and after

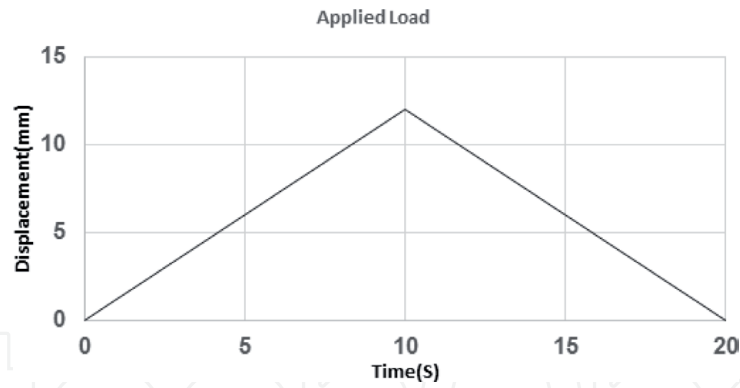


Figure 4.
 The quasi-static loading/unloading on the SMA specimen by MTS machine.

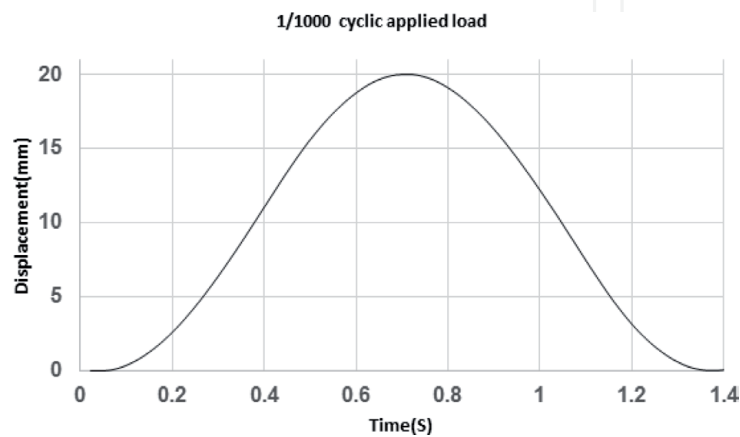


Figure 5.
 The first loading cycle on SMA specimen in cyclic loading.

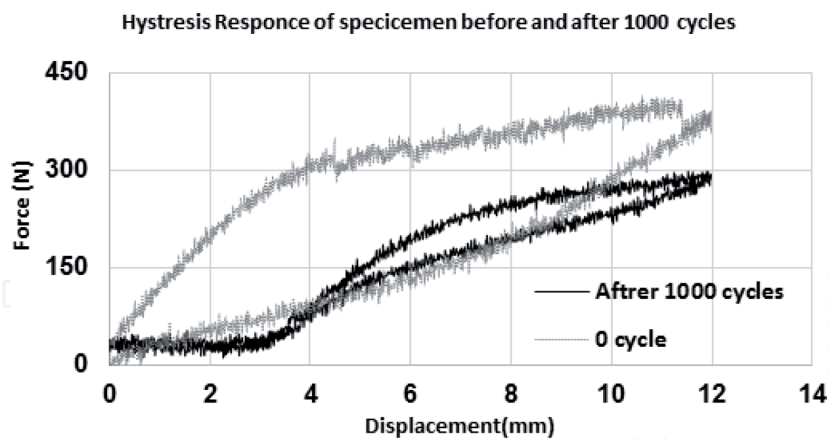


Figure 6.
 The effect of cyclic loading on force-displacement.

1000 load cycles are shown in **Figure 6**, in which 0 cycle stands for the quasi-static loading described in **Figure 4**. After 1000 load cycles, two major impacts on the force-displacement curve of SMA are realized, a significant reduction on hysteresis which, in turn, results in reduction in energy absorption, and reduction in material properties, E_A and E_M . Reduction in material properties is mainly due to the degradation phenomena of SMA. The effect of cyclic loading/unloading on material properties, E_A and E_M , are presented as a correction factor of the ratio of E after 1000 cycle (E_{1000}) and E when the specimen is subjected to a single quasi-static load (E_0), in **Figure 6**. After 1000 cycles, E_A shows 18% reduction, whereas E_M 33% compared to the initial single quasi-static loading condition.

3.2 Effect of pre-straining on SMA properties

Long-term stability and performance of civil structures under dynamic loadings is an essential feature for many applications. Therefore, structural designers do not tolerate the change in structural strength and stability. As it was realized in the previous section, cyclic load results in a significant reduction in material properties and, in turn, a reduction in the stability and loading characteristics of SMA-based structural elements.

In order to mitigate the negative effect of cyclic loading on SMA-based elements, 10 mm initial displacement is applied to the SMA wire, which is far beyond the elastic displacement region, and 10 mm is approximately equal to 1.7% pre-strain. The hysteresis response of 1.7% pre-strained SMA wire subjected to the loading protocol, as presented in Figure 5, after 1000 cycles, is given in Figure 7. Comparison of Figure 7 and Figure 6 exhibits that pre-straining SMA eliminates the residual deformation occurred after 1000 cyclic load/unloading.

Figure 8 provides the comparison between E_A and E_M of the specimen after applying 1000 cyclic loads. It is noted that pre-straining improves the value of E_A from 82% at 0% pre-strain to 52% at 1.7% pre-straining the specimen. However, 1.7% pre-straining completely return the value of E_M from 67% at 0% to its initial state.

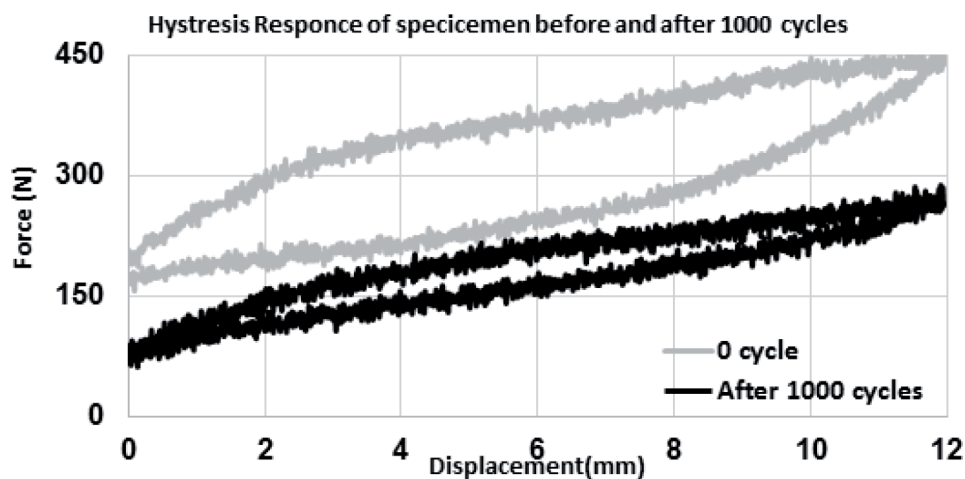


Figure 7.
The hysteresis response of 1.7% pre-strain specimen after applied 1000 cycles.

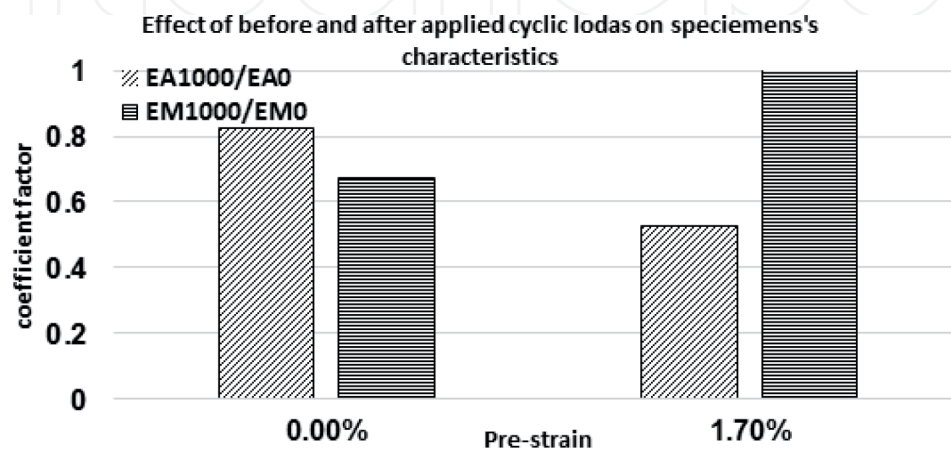


Figure 8.
The effect of applied cyclic loading on characteristics of 0 and 1.7% pre-strain specimen.

3.3 Effect of pre-straining and sequentially increasing load on SMA properties

Sequentially increasing loadings is a common loading profile for many civil applications including offshore structures, requiring a thorough understanding of the response of structures under such loading profile. In this section, two specimens are exposed to a sequentially increasing quasi-static loading protocol as presented in **Figure 9**. It composes of four cycles with 20 s period and arbitrary amplitude of 11.61 mm (called loading sequence (LS) 1), 13.58 mm (called loading sequence (LS) 2), 17.51 mm (called loading sequence (LS) 3), and 19.48 mm (called loading sequence (LS) 4), respectively. Two parameters, namely, E_A and E_M , have been studied again under this loading protocol. Then, the loading profile is repeated for 1000 cycles, and the response of the specimens is recorded. Similar to the constant loading profile, it is observed that cyclic load leads to a significant reduction in material properties, E_A and E_M . In another experiment, the specimens are subjected to 1.7% pre-straining where it revealed a significant improvement in the material properties. As shown in **Figure 10**, applying a value of 1.7%, pre-strain changes the value of the correction factor E_{A1000}/E_{A0} from 62% (for the first period) to 81% (for the fourth period) to 52 and 72%, correspondingly. In a similar observation, applying a value of 1.7%, pre-straining changes the value of the correction factor E_{M1000}/E_{M0} from 67 to 54%.

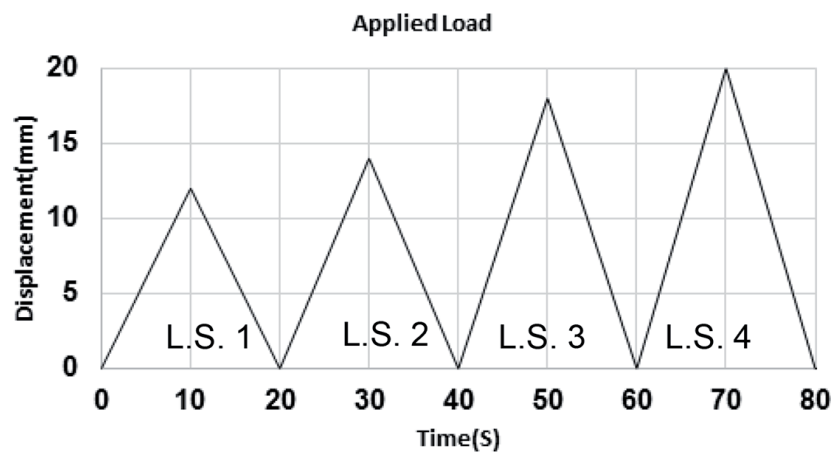


Figure 9.
 The loading protocol for 0 and 1.7% pre-strain specimen.

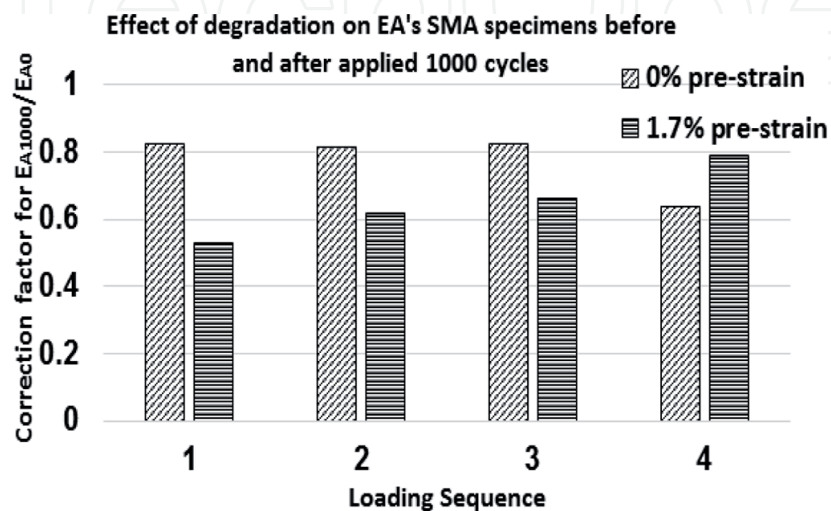


Figure 10.
 The effect of cyclic loading on E_A of 0 and 1.7% pre-strain specimen.

4. Correction factor for stress-strain of SMA under cyclic loadings

Close study of force-displacement curves for SMA specimen subjected to cyclic loading, and pre-straining reveals that the number of cycles and pre-straining significantly influences the predetermined stress-strain behavior of SMA-based structural elements. In many applications the structure undergoes dynamic loadings, requiring an accurate yet practical estimation of the effect of loading conditions, on the performance and functionality of the structure for long-term usage. According to the present experimental results, practical correction factors are introduced to estimate the effects of cyclic. According to the present experimental results, it is realized that the change in E_M and E_A is a function of correction factors relating cyclic loading, pre-straining, and initial material properties as the following:

$$E_A'' = f(\alpha, \beta, E_A), E_M'' = f(\alpha', \beta', E_M) \quad (5)$$

where α and α' are the correction factors relating E_{A1000}/E_{A0} and E_{M1000}/E_{M0} . Similarly β and β' are correction factors relating E_{A1000} at 1.7% pre-straining / E_{A1000} at 0% pre-straining and E_{M1000} at 1.7% pre-straining / E_{M1000} at 0% pre-straining. The terms E_A'' and E_M'' indicate corrected value for E_A and E_M as a result of cyclic loading and pre-straining. Accordingly, the functions relating E_A'' to E_A and E_M'' to E_M can be estimated as:

$$E_A'' = \alpha\beta E_A, E_M'' = \alpha'\beta' E_M \quad (6)$$

The correction factors, $\alpha\beta$ and $\alpha'\beta'$ are presented in **Figures 10** and **11**. The values for α and α' are given in **Figure 12**.

As observed in the conventional specimen (0% pre-straining), β and β' are assumed 1. Hence, Eq. (6) is now modified to:

$$E_A'' = \alpha E_A, E_M'' = \alpha' E_M \quad (7)$$

where $\alpha \approx 0.6 - 0.81$ and $\alpha' \approx 0.6 - 1.2$.

In the case of applied 1.7% pre-straining, coefficients in Eq. (6) can be calculated by $\alpha\beta \approx 0.45-0.8$ and $\alpha'\beta' \approx 0.56 - 0.98$.

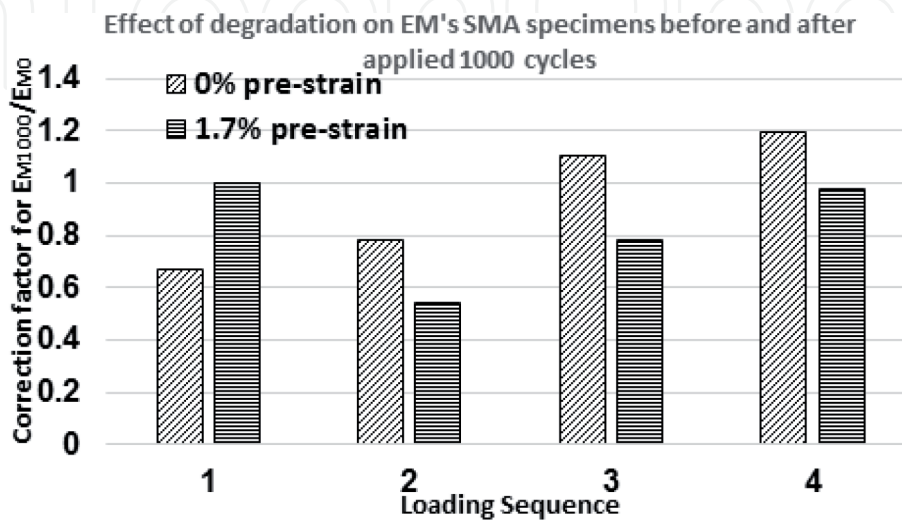


Figure 11.
The effect of cyclic loading on E_M of 0 and 1.7% pre-strain specimen.

Considering the effects of cyclic loading and pre-straining on stress-strain behavior of SMA wires, **Figure 13(a)** is now modified to **Figure 13(b)**, where one may realize a significant reduction in critical stress-strain points as well as changes in residual strain after cyclic loading.

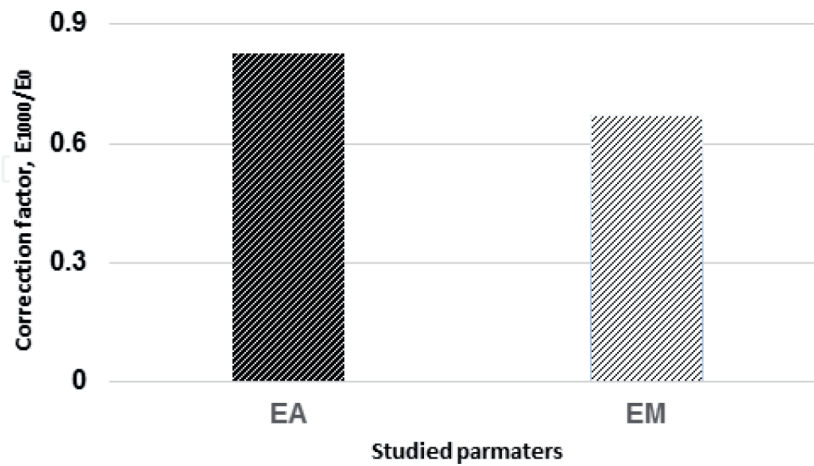


Figure 12.
 The effect of applied cyclic loading on EA and EM.

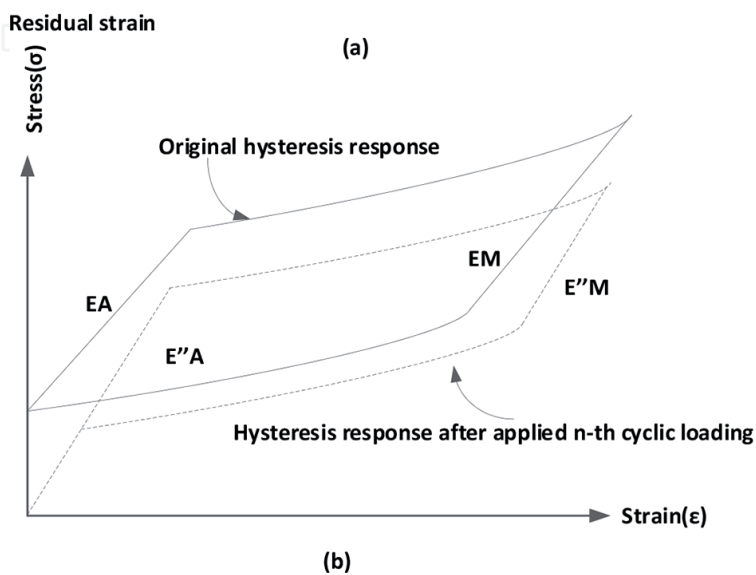
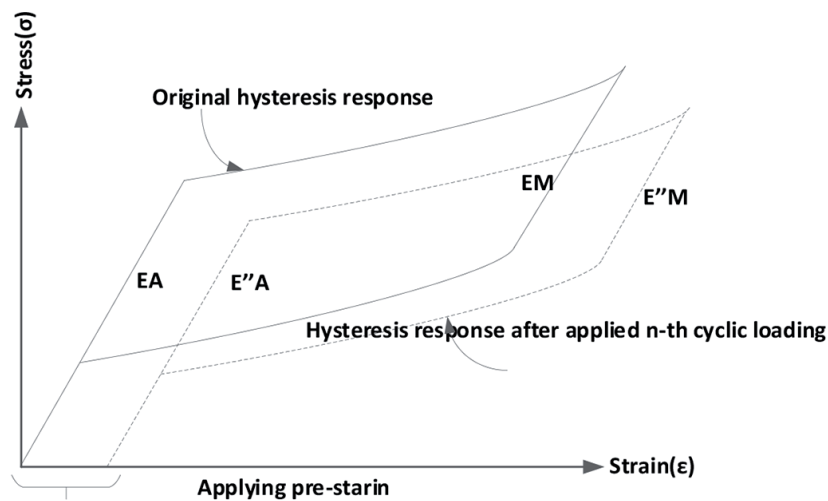


Figure 13.
 The effect of cyclic loading (a) 0% pre-strained SMA (b) 1.7% pre-strained SMA on EA and EM.

5. Conclusions

The effects of cyclic loading and pre-straining on stress-strain behavior of SMA wires have been investigated. Several experimental tests have been conducted to study the effects of the number of cycles and pre-straining on strain recovery and modulus of elasticity of SMA wires. Correction factors have been provided to encounter the effects of cyclic loads and pre-straining on stress-strain behavior of SMA wires. It is observed that cyclic loading may lead to huge residual strain and reduces the strain recovery feature of SMA. However, pre-straining SMA for only 1.7% significantly improves the reduction in strain recovery of SMA as a result of cyclic loading.

Acknowledgements

This research received funding from the Green Construction Research and Training Center (GCRTC). The authors wish to thank the University of British Columbia-Okanagan Campus, for the technical support. The authors also wish to thank Mr. Kyle Charles as a research engineer and ex lab manager for his valuable help in experimental tests at the applied laboratory for advanced materials and structures at the University of British Columbia-Okanagan Campus.

Author details


Shahin Zareie^{1*} and Abolghassem Zabihollah²

¹ School of Engineering, The University of British Columbia, Kelowna, BC, Canada

² School of Science and Engineering, Sharif University of Technology, International Campus, Kish Island, Iran

*Address all correspondence to: shahin@alumni.ubc.ca

IntechOpen

© 2020 The Author(s). Licensee IntechOpen. Distributed under the terms of the Creative Commons Attribution - NonCommercial 4.0 License (<https://creativecommons.org/licenses/by-nc/4.0/>), which permits use, distribution and reproduction for non-commercial purposes, provided the original is properly cited. 

References

- [1] Aryan H, Ghassemieh M. A superelastic protective technique for mitigating the effects of vertical and horizontal seismic excitations on highway bridges. *Journal of Intelligent Material Systems and Structures*. 2017;**28**(12):1533-1552
- [2] Zareie S, Mirzai N, Alam MS, Seethlaer RJ. A dynamic analysis of a novel shape memory alloy-based bracing system. In: CSCE 2017; 2017
- [3] Zareie S, Mirzai N, Alam MS, Seethlaer RJ. An introduction and modeling of novel shape memory alloy-based bracing. In: CSCE 2017; 2017
- [4] Zareie S, Alam MS, Seethaler RJ, Zabihollah A. An experimental study of SMA wire for tendons of a tension leg platform. In: 5th Annual Engineering Graduate Symposium; 2019
- [5] Zareie S, Shahria Alam M, Seethlaer RJ, Zabihollah A. Effect of shape memory alloy-magnetorheological fluid-based structural control system on the marine structure using nonlinear time-history analysis. *Journal of Applied Ocean Research*. 2019;**91**:101836
- [6] Zareie S, Shahria Alam M, Seethlaer RJ, Zabihollah A. An experimental study of SMA wire for tendons of a tension leg platform. In: 5th Annual Engineering Graduate Symposium; 2019
- [7] Zareie S, Alam MS, Seethaler RJ, Zabihollah A. Effect of cyclic loads on SMA-based component of cable-stayed bridge. In: 7th International Specialty Conference on Engineering Mechanics and Materials; 2019
- [8] Miyazaki S, Imai T, Igo Y, Otsuka K. Effect of cyclic deformation on the pseudoelasticity characteristics of Ti-Ni alloys. *Metallurgical Transactions A*. 1986;**17**(1):115-120
- [9] Zhang Y, Zhu J, Moumni Z, Van Herpen A, Zhang W. Energy-based fatigue model for shape memory alloys including thermomechanical coupling. *Smart Materials and Structures*. 2016;**25**(3):35042
- [10] Yu C, Kang G, Kan Q, Song D. A micromechanical constitutive model based on crystal plasticity for thermo-mechanical cyclic deformation of NiTi shape memory alloys. *International Journal of Plasticity*. 2013;**44**:161-191
- [11] Wang W, Chan T-M, Shao H, Chen Y. Cyclic behavior of connections equipped with NiTi shape memory alloy and steel tendons between H-shaped beam to CHS column. *Engineering Structures*. 2015;**88**:37-50
- [12] Chemisky Y, Chatzigeorgiou G, Kumar P, Lagoudas DC. A constitutive model for cyclic actuation of high-temperature shape memory alloys. *Mechanics of Materials*. 2014;**68**:120-136
- [13] Kan Q, Yu C, Kang G, Li J, Yan W. Experimental observations on rate-dependent cyclic deformation of super-elastic NiTi shape memory alloy. *Mechanics of Materials*. 2016;**97**:48-58
- [14] Soul H, Isalgue A, Yawny A, Torra V, Lovey FC. Pseudoelastic fatigue of NiTi wires: Frequency and size effects on damping capacity. *Smart Materials and Structures*. 2010;**19**(8):85006
- [15] DesRoches R, McCormick J, Delemont M. Cyclic properties of superelastic shape memory alloy wires and bars. *Journal of Structural Engineering*. 2004;**130**(1):38-46
- [16] Leo DJ. *Engineering Analysis of Smart Material Systems*. John Wiley & Sons; 2007

[17] Zuo X-B, Li A-Q, Sun W, Sun X-H.
Optimal design of shape memory alloy
damper for cable vibration control.
Journal of Vibration and Control.
2009;15(6):897-921

IntechOpen

IntechOpen